IEEE Access
Multidisciplinary | Rapid Review | Open Access Journal

Date of publication xxxx 00, 0000, date of current version xxxx 00, 0000.

Digital Object Identifier 10.1109/ACCESS.2017.Doi Number

Demand-side power paradigm-oriented analysis of reactive electric spring stabilization capabilities

Giuseppe Buja[1], Life Fellow, IEEE, Stefano Giacomuzzi[1], Student Member, IEEE, Qingsong Wang[2], Senior Member, IEEE, and Manuele Bertoluzzo[1]

[1]Department of Industrial Engineering, University of Padova, 35131 Padova, Italy
[2]School of Electrical Engineering, Southeast University, 2 SiPaiLou, Nanjing 210096, China

Corresponding author: Stefano Giacomuzzi (stefano.giacomuzzi@phd.unipd.it).

ABSTRACT Electric Spring (ES) technique is a user-level solution developed to stabilize the supply voltage of a user under variations of the grid voltage. This paper analyzes the stabilization capabilities of a reactive ES that operates according to the demand-side power paradigm. By help of a convenient ES modeling, the extreme values of the active power that a user can draw under the ES action are first determined. Then, it is demonstrated that the demand-side power paradigm is fulfilled only if the distribution line impedance has a resistive component while its reactive component weakens such fulfillment. Lastly, the variations of the grid voltage that ES is able to cope with are worked out. All findings are formulated in terms of normalized quantities and consequently are of general validity. Computer-aided simulation of a case study exemplifies the theoretical findings.

INDEX Electric Spring, Voltage Stabilization, Smart Grid, Distribution Network, Distribution Generation.

I. INTRODUCTION

The increased grid proliferation of renewable energy sources (RESs) is liable to impair the quality of the electric service. Indeed, the fluctuations of the grid power due to the intermittency of RESs cause the variation of the grid voltage feeding the distribution lines and this, in turn, deviates the supply voltage of a user from the nominal value. Various solutions have been developed to stabilize such a voltage [1]. They can be deployed at two levels: distribution-level and user-level [2].

Electric Spring (ES) technique is a recently developed user-level solution. Conceptualized by Hui et al. in [3], the ES technique is the electric version of the Hooke's law for a mechanical system [4]. The concept behind it can be briefly explicated as follows. The user loads are separated into two sets, namely the set that tolerates a certain deviation of the supply voltage, termed as Non-Critical Load (NCL), and the set that needs a nearly constant supply voltage, termed as Critical Load (CL). An ES circuitry, hereafter simply termed as ES, modifies the voltage across and -then- the current through NCL so as to keep constant, i.e. to stabilize, the CL voltage at the nominal value under grid voltage variations. This entails that the active power drawn by CL remains constant while that one drawn by NCL changes.

Fig.1 illustrates the schematic of a single-phase user equipped with ES and connected to a distribution line at supply point S. CL is directly connected to S whilst NCL is connected to S through ES. The circuitry of ES is comprising of a PWM voltage source inverter (VSI), filtering inductance L_f and capacitor C_{ES}. The branch formed by ES and NCL is called Smart Load (SL) and its terminal voltage, given by the sum of voltage v_{ES} across the capacitor and voltage v_{NCL} across NCL, is just the user voltage v_S. By properly commanding VSI, voltage v_{ES} is driven to stabilize the magnitude of v_S despite the variations of the grid voltage. Therefore, CL is supplied at the nominal voltage whilst NCL, due to the presence of v_{ES}, is no more.

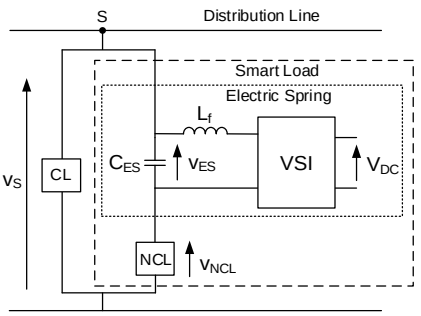

FIGURE 1. **Schematic of a single-phase user equipped with ES.**

This article has been accepted for publication in a future issue of this journal, but has not been fully edited. Content may change prior to final publication. Citation information: DOI 10.1109/ACCESS.2020.3040292, IEEE Access

Two topologies have been originally devised to implement ES, namely reactive and active [5]. In the reactive ES, a capacitor is utilized at the DC input of VSI and the user voltage stabilization is achieved thanks to the reactive power made available by ESs [6], [7]. Instead, in the active ES, a battery is utilized at the DC input of VSI and the user voltage stabilization is achieved thanks to both active and reactive powers made available by ES [8]. The reactive ES is cost effective and dispenses of most maintenance tasks. The active one allows the execution of additional services in favor of the grid such as correction of the power factor [9]-[11].

In [12], the two above-mentioned topologies are respectively referred to as ES-1 and ES-2. In addition to them, ESs with other active topologies have been proposed during the last years, like the back-to back (B2B) ES, where a back-to-back converter is incorporated into the ES circuitry to avoid the use of any battery in the DC voltage link [13], and the RES-integrated ES, where a photovoltaic (PV) panel supplies ES [14]. This paper is concerned with the ES-1 topology, i.e. with the reactive ES.

Application of ES for the stabilization of the user voltage enables to fulfill the demand-side power paradigm in an electric system. As know, in contrast to the traditional supply-side power paradigm, the demand-side one provides for adapting the demand of power to the generation. Notwithstanding this potential of ES application, the existing literature [15]-[17] has not carried out yet an analysis of the user voltage stabilization capabilities of ES that is operated according to the demand-side power paradigm.

The purpose of this paper is to perform such an analysis for a user equipped with a reactive ES (hereafter designated with RESE user) by giving for grant that an excess of power generation produces an overvoltage of the grid feeding the distribution lines whilst a shortage of power generation produces an undervoltage of it. Videlicet, the paper examines the stabilizing action of a reactive ES under the constraint that the active power drawn by NCL tracks the fluctuations of the power generation; this means that, under an excess of power generation, the ES action must be consistent with NCL that draws an active power greater than its nominal value and vice versa.

From the grid point of view, the fulfillment of the demand-side power paradigm would facilitate the integration of distributed RESs since it modifies the power consumption according to the supply conditions. Several papers have recently analyzed the possible impact of ESs on the distribution grid, but the demand-side power paradigm concept has never been addressed. For example, in [18] it is demonstrated that, for different lengths and R/X ratios of a distribution line, the ES installation at different locations from a substation is not an issue for the network stability. In [19] and [20], an optimal ES allocation is suggested with the objective of minimizing the user voltage deviation, but no mention is done about any demand-side power behavior for the optimal operation of the electric system. In [21], ES is inserted in series to the whole user load and its action is intended to limit the deviation of the user load voltage within ±5%; as a consequence, the CL voltage can also deviate within this range, ignoring the distinct voltage needs of CL and NCL. The objective is to provide a load-side virtual inertia through the power reserve that comes from the ±5% deviation of the nominal load voltage. This means that ES is no more utilized to stabilize the CL voltage, but to improve the primary frequency response by the increase of the power system inertia. Paper [22] compares the stabilization capabilities of a reactive ES with those of the active ESs, in particular of B2B ES, finding out that the equivalent R/X ratio of the distribution line plays an important role in the user voltage regulation exerted by SLs. It is shown that the voltage variations in grids with high PV and Electric Vehicle (EV) penetration increase for higher R/X ratio since both PVs and EVs exchange only active power with the grid; however, it is not considered the effect of the R/X ratio on the demand-side power response.

This paper is organized in VII Sections. Section II explains the modus operandi pursued in the analysis of the operation of a RESE user and conceives an ES model useful to describe its action. Section III calculates the extreme values of the active power range that NCL draws under the ES action. Section IV investigates the voltage drop along a distribution line. Section V determines the voltage stabilization range achievable by a RESE user against the grid voltage variations while fulfilling the demand-side power paradigm; moreover, it highlights that the stabilization range strongly depends on the resistive component of the distribution line impedance. The theoretical findings are expressed analytically by help of normalized quantities and, thus, constitute a general tool for a user to evaluate the stabilization capabilities offered by the ES installation. Section VI presents a case study to exemplify the theoretical findings. Section VII concludes the paper.

Throughout the paper, the following conventions are used: nominal conditions refer to the situation with no variations of the grid voltage; the relevant quantities are denoted by subscript N. Upper-case letters overmarked with a bar denote phasors; those overmarked with a point denote impedance whilst those without any overmark denote magnitude of the respective quantities. Subscripts Max and Min denote respectively maximum and minimum magnitudes of the quantities under the ES action. The normalized quantities are expressed as a fraction of the respective magnitudes in nominal conditions.

II. ES DESCRIPTION

The electric scheme of a single-phase RESE user is illustrated in Fig. 2, together with the supplying distribution line. In the figure, voltage v_G and current i_G are quantities related to the grid whilst resistance R_G and inductance L_G are related to the distribution line. Voltages v_{CL} and v_{NCL}, currents i_{CL} and i_{NCL}, resistances R_{CL} and R_{NCL}, and inductances L_{CL} and L_{NCL} are quantities related to CL and NCL, respectively. Capacitor C and voltage V_{DC} are quantities related to the DC

This article has been accepted for publication in a future issue of this journal, but has not been fully edited. Content may change prior to final publication. Citation information: DOI 10.1109/ACCESS.2020.3040292, IEEE Access

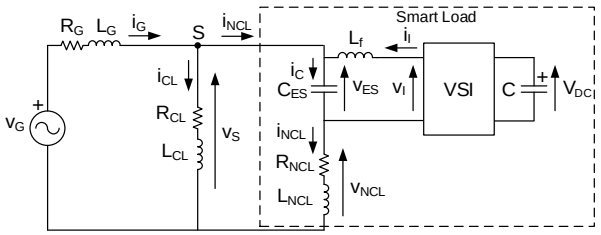

FIGURE 2. Electric scheme of a single-phase RESE user.

input stage of ES whilst capacitor C_{ES}, inductance L_f, voltage v_I, current i_I and voltage v_{ES} are related to the AC output stage of ES. Note that current i_C entering in C_{ES} is the sum of i_{NCL} and i_I whilst the current entering in SL is just i_{NCL}.

A. ES OPERATION

The analysis presented in this paper relies on the behavior of the circuit in Fig. 2 at sinusoidal steady state; therefore, the fundamental components are taken for the VSI output voltage and current. In nominal conditions, current i_I equates i_{NCL} in magnitude and opposes to it in phase; then both i_C and v_{ES} are zero and ES does not exert any action on the user supply. Further to a grid voltage variation, ES acts by adjusting v_{ES} in order to stabilize the magnitude of v_S. Since ES is reactive, the adjustment of v_{ES} is attained by changing the magnitude of i_I while its phase is kept in quadrature to v_{ES}. This implies that i_I is, in principle, either in phase or in phase opposition to i_{NCL}, as expressed in phasor form by

$$\bar{I}_I = -a\,\bar{I}_{NCL} \tag{1}$$

where a is a real number. In practice, i_I is in phase opposition to i_{NCL} and a in (1) is a positive number that goes from values greater than 1 to 0, being equal to 1 in nominal conditions.

The adjustment of v_{ES} modifies both magnitude and phase of v_{NCL} with respect to v_S and the same occurs for the active and reactive powers drawn by NCL; for a reactive ES, the active power drawn by NCL is equal to that drawn by SL whilst this does not hold for the reactive power; specifically, for i_{NCL} lagging v_{ES}, the reactive power absorbed by C_{ES} adds to that of NCL; for i_{NCL} leading v_{ES}, it subtracts from that of NCL and, if greater than that of NCL, makes the reactive power absorbed by SL of capacitive type.

B. MODUS OPERANDI

Analysis of the scheme of Fig. 2 is performed by assuming that ES keeps V_S steadily at $V_{S,N}$ under grid voltage variations.

C. ES MODELING

By (1), the voltage across C_{ES} can be written as

$$jX_{CES}\bar{I}_C = jX_{CES}(1-a)\bar{I}_{NCL} \tag{2}$$

where X_{CES} in (2) is equal to

$$X_{CES} = -\frac{1}{\omega C_{ES}} \tag{3}$$

and ω in (3) is the grid angular frequency. The term on the right-hand side of (2) shows that ES can be modeled with the equivalent reactance

$$X_{eq} = X_{CES}(1-a) \tag{4}$$

flowed by current $\bar{I}_{NCL}$ and, hence, placed in series to NCL. Nature (inductive or capacitive) and value of X_{eq} depend on the ratio a in (1). Eq. (4) substantiates what anticipated before: for a=1, X_{eq} is 0, signifying that ES action does not interfere in the NCL operation; for a ranging from 1 to 0, X_{eq} is less than 0 and the ES action is of capacitive type; for a greater than 1, X_{eq} is greater than 0 and the ES action is of inductive type.

By (4), the scheme of Fig. 2 can be represented as in Fig. 3 (a), where $\dot{Z}_G$, $\dot{Z}_{CL}$ and $\dot{Z}_{NCL}$ are the impedances of the distribution line, CL and NCL, respectively. The SL branch can also be represented in more detail as in Fig. 3 (b), where $\bar{V}_{X,SL}$ is the voltage across the total SL reactance, given by the sum of X_{eq} and X_{NCL}. Inspection of Fig. 3 (b), the reactive nature of X_{eq} and the change of its value with a yield that

i. phase φ_{SL} of the SL impedance changes further to the ES action, being equal to that of NCL, i.e. to φ_{NCL}, in nominal conditions,
ii. the power factor of SL increases for a ranging from 1 to 0, and decreases for a greater than 1; incidentally, the latter inconvenience is circumvented by resorting to active ESs.

III. NCL-DRAWN ACTIVE POWER EXTREME VALUES

Power P_{NCL} drawn by NCL in nominal conditions is equal to

$$P_{NCL,N} = \frac{(V_{S,N}\cos\varphi_{NCL})^2}{R_{NCL}} \tag{5}$$

Maximum power $P_{NCL,Max}$ drawn by NCL is reached when voltage $V_{R,NCL}$ across R_{NCL} is equal to $V_{S,N}$. As shown by the diagram with red phasors in Fig. 4, in this circumstance it occurs that i) $\bar{V}_{ES}$ exactly opposes to the voltage drop across X_{NCL} so that voltage $\bar{V}_{X,SL}$ is zero, and ii) the phase of the SL impedance is also zero, which means that SL works at unity power factor. Note that an additional increase of $\bar{V}_{ES}$ would reduce $V_{R,NCL}$ and, with it, the active power drawn by NCL. In

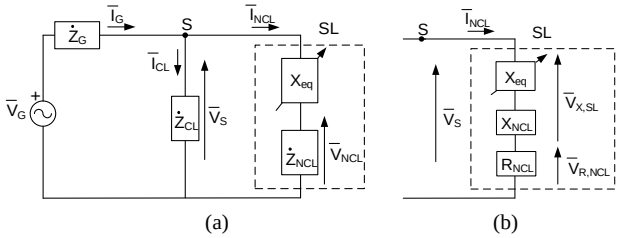

FIGURE 3. (a) Equivalent representation of the scheme in Fig. 2; (b) detailed SL branch representation.

This article has been accepted for publication in a future issue of this journal, but has not been fully edited. Content may change prior to final publication. Citation information: DOI 10.1109/ACCESS.2020.3040292, IEEE Access

correspondence to $P_{NCL,Max}$, both voltage $V_{R,NCL}$ and current I_{NCL} get their maximum magnitudes, denoted as $V_{R,NCL,Max}$ and $I_{NCL,Max}$.

The value of $P_{NCL,Max}$ normalized to $P_{NCL,N}$ is

$$P_{NCL,Max} = \frac{1}{(cos\varphi_{NCL})^2} \tag{6}$$

The values of $V_{R,NCL,Max}$ and $I_{NCL,Max}$, normalized to the respective magnitudes in nominal conditions, are equal to $1/cos\varphi_{NCL}$. These outcomes are collected in Tab. I for $cos\varphi_{NCL} = 0.9$.

In principle, the minimum power that NCL could draw is zero and is reached when $\bar{V}_{ES} = \bar{V}_{S,N}$. Nevertheless, it is commonly requested to energize NCL -even if at reduced power- also under an undervoltage, as shown by the diagram with blue phasors in Fig. 5. Let the minimum power $P_{NCL,Min}$ drawn by NCL be set at a percentage A of $P_{NCL,N}$; the resultant power factor of SL is

$$\left(cos\varphi_{SL,Min}\right)^2 = A(cos\varphi_{NCL})^2 \tag{7}$$

In correspondence to (7), also $V_{R,NCL}$ and I_{NCL} get minimum magnitudes, denoted as $V_{R,NCL,Min}$ and $I_{NCL,Min}$; their normalized values are equal to $cos\varphi_{SL,Min}/cos\varphi_{NCL} = \sqrt{A}$. These outcomes are collected in Tab. I for A=62% and $cos\varphi_{NCL} = 0.9$. Note that, for the chosen value of A, the power factor of SL when drawing $P_{NCL,Min}$ is $1/\sqrt{2}$.

IV. LINE VOLTAGE DROP STUDY

A. LINE VOLTAGE DROP CALCULATION

Magnitude V_{DL} of the voltage drop along a distribution line is given by

$$V_G = V_{DL} + V_S \tag{8}$$

As per the IEC standards [23], it is well approximated by

$$V_{DL} = R_G\, I_{G,a} + X_G\, I_{G,r} \tag{9}$$

where $I_{G,a}$ and $I_{G,r}$ are the projections of $\bar{I}_G$ respectively along the direction of $\bar{V}_S$ and that one of an axis rotated of -π/2 out of $\bar{V}_S$. The two projections are the so-called active and reactive components of $\bar{I}_G$ and are equal to the sum of the respective

TABLE I
SL ELECTRIC QUANTITIES EXTREME VALUES

Case	Magnitude	Normalized Value
Nominal	$P_{NCL,N}$	1
	$V_{NCL,N}$, $I_{NCL,N}$	1
Maximum	$P_{NCL,Max}$	1.23
	$V_{NCL,Max}$, $I_{NCL,Max}$	1.11
Minimum	$P_{NCL,Min}$	0.62
	$V_{NCL,Min}$, $I_{NCL,Min}$	0.78

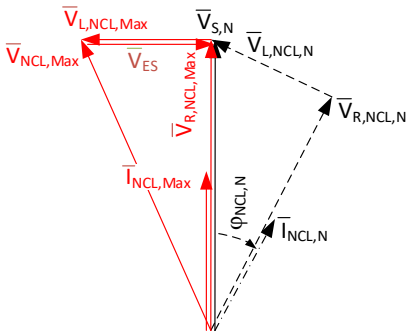

FIGURE 4. SL phasor diagram for the maximum active power drawn by NCL. SL phase $\varphi_{SL,Max}$, not reported in the diagram, is zero.

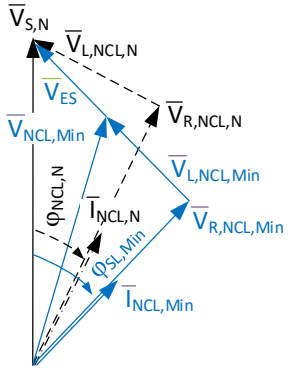

FIGURE 5. SL phasor diagram for the set value of the minimum active power drawn by NCL.

components of the CL and NCL currents

$$I_{G,a} = I_{NCL,a} + I_{CL,a} \qquad I_{G,r} = I_{NCL,r} + I_{CL,r} \tag{10}$$

By (8), the user voltage stabilization is attained as long as the variations of V_G are counterbalanced by equal variations of V_{DL}. For V_S steadily at $V_{S,N}$, the active and reactive components of $\bar{I}_{CL}$ remain unaltered and the stabilization of V_S can be obtained only by modifying the active and reactive components of $\bar{I}_{NCL}$. Rewriting (8) and (9) under V_G variations leads to

$$\Delta V_G = \Delta V_{DL} \tag{11}$$

$$\Delta V_{DL} = R_G\, \Delta I_{NCL,a} + X_G \Delta I_{NCL,r} \tag{12}$$

where the variational quantities in (11) and (12) are taken with respect to the relevant nominal values. By (11), the range of ΔV_G that can be stabilized depends on the achievable values of ΔV_{DL}; by (12), the latter values depend on the components of the distribution line impedance and the achievable variations, sign included, of the active and reactive components of $\bar{I}_{NCL}$.

For the demand-side power paradigm to be fulfilled, the sign of $\Delta I_{NCL,a}$ must be the same as ΔV_G, i.e. it must be excluded the circumstance by which $\Delta I_{NCL,a}$ varies in opposition to ΔV_G and the balance in (12) is reached thanks to the variations of $\Delta I_{NCL,r}$. In other words, let ΔV_G be positive;

This article has been accepted for publication in a future issue of this journal, but has not been fully edited. Content may change prior to final publication. Citation information: DOI 10.1109/ACCESS.2020.3040292, IEEE Access

the counterbalancing value of ΔV_{DL} must not be obtained with a negative one of $\Delta I_{NCL,a}$ and a positive value of $\Delta I_{NCL,r}$ and the concurrent prevalence of the absolute value of the voltage drop across the line reactance with respect to the line resistance. This represents the constraint to be imposed for the fulfillment of the demand-side power paradigm when stabilizing the user voltage and is taken on in the next Section.

B. NCL CURRENT COMPONENTS

The SL voltage is comprised of two phasors, namely resistive phasor $\bar{V}_{R,NCL}$ and reactive phasor $\bar{V}_{X,SL}$. The two phasors are orthogonal, and their sum gives $\bar{V}_{S,N}$. Changing of the reactive phasor ensuing from the adjustment of X_{eq} makes the tip of $\bar{V}_{R,NCL}$ to describe a semi-circumference whose diameter is $V_{S,N}$, as traced in Fig. 6. The same is done by the tip of $\bar{I}_{NCL}$, the diameter of its semi-circumference being $V_{S,N}/R_{NCL}$.

When the tip of $\bar{V}_{R,NCL}$ moves from NV to PV, the tip of $\bar{I}_{NCL}$ moves from NI to PI. This motion is outlined by the SL phasors traced with solid red arrows in Fig. 6, where NV and NI are the tips of $\bar{V}_{S,N}$ and $\bar{I}_{NCL}$ in nominal conditions and PV and PI are their tips under the situation of maximum active power drawn by NCL. While $\bar{I}_{NCL}$ moves towards PI, $I_{NCL,a}$ increases whilst $I_{NCL,r}$ decreases; hence $\Delta I_{NCL,a}$ takes a positive value whilst $\Delta I_{NCL,r}$ takes a negative value.

In the dual way, when the tip of $\bar{V}_{R,NCL}$ moves from NV to QV, the tip of $\bar{I}_{NCL}$ moves from NI to QI, where QV and QI are the tips of $\bar{V}_{R,NCL}$ and $\bar{I}_{NCL}$ under the situation of minimum power drawn by NCL as defined in the previous Section. This motion is outlined by the SL phasors traced with solid blue arrows in Fig. 6. While $\bar{I}_{NCL}$ moves towards QI, $I_{NCL,a}$ decreases whilst $I_{NCL,r}$ increases; hence, $\Delta I_{NCL,a}$ takes a negative value whilst $\Delta I_{NCL,r}$ takes a positive value.

The variations $\Delta I_{NCL,a}$ and $\Delta I_{NCL,r}$ as a function of the variation ΔP_{NCL} of the active power drawn by NCL are plotted in Fig. 7, where all the quantities are normalized. The plot of $\Delta I_{NCL,a}$ reveals that

i. it has the same sign as ΔP_{NCL},
ii. it varies proportionally to ΔP_{NCL} as one readily deduces from (13) by reminding that $V_{S,N}$ is constant.

$$I_{NCL,a} = \frac{1}{V_{S,N}} P_{NCL} \tag{13}$$

In normalized form, $\Delta I_{NCL,a}$ as a function of ΔP_{NCL} is given by

$$\frac{\Delta I_{NCL,a}}{I_{NCL,a,N}} = \frac{\Delta P_{NCL}}{P_{NCL,N}} \tag{14}$$

The plot of $\Delta I_{NCL,r}$ reveals that

i. it is positive when ΔP_{NCL} is negative and vice versa,
ii. it varies inversely to ΔP_{NCL} as one readily deduces from (15), being the rate of change of $tan\varphi_{SL}$ opposite to that of P_{NCL}

$$I_{NCL,r} = \frac{tan\varphi_{SL}}{V_{S,N}} P_{NCL} \tag{15}$$

In normalized form, $\Delta I_{NCL,r}$ as a function of ΔP_{NCL} is given by

$$\frac{\Delta I_{NCL,r}}{I_{NCL,r,N}} = \frac{tan\varphi_{SL} P_{NCL}}{tan\varphi_{NCL} P_{NCL,N}} - 1 \tag{16}$$

whereas angle φ_{SL} can be expressed as

$$\varphi_{SL} = arcos\sqrt{cos^2\varphi_{NCL} + \frac{R_{NCL}}{V_{S,N}^2}\Delta P_{NCL}} \tag{17}$$

Putting together (11), (14) and (16) yields the two following leading outcomes:

i. only a distribution line with a resistive component of its impedance may allow the fulfilment of the demand-side power paradigm. If the distribution line is purely resistive (R-line), the paradigm is surely fulfilled while it is never fulfilled for a purely reactive line,

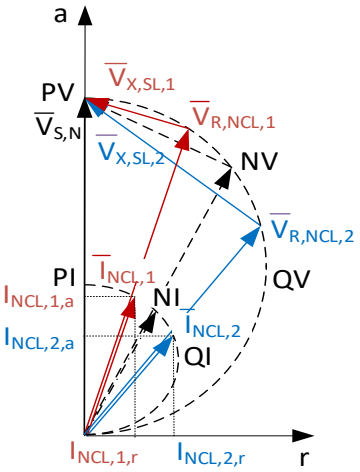

FIGURE 6. SL phasor diagram under various values of active power drawn by NCL.

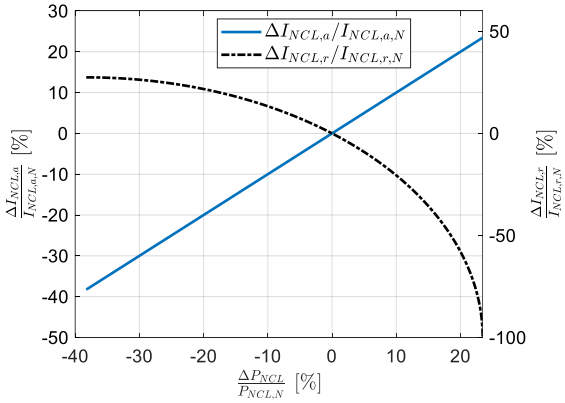

FIGURE 7. NCL active and reactive current components vs. NCL-drawn active power: variational quantities.

This article has been accepted for publication in a future issue of this journal, but has not been fully edited. Content may change prior to final publication. Citation information: DOI 10.1109/ACCESS.2020.3040292, IEEE Access

ii. a distribution line with mixed resistive-inductive impedance (RL-line) allows the fulfilment of the demand-side power paradigm only if the following constraint is met:

$$R_G \left|\Delta I_{NCL,a}\right| > X_G \left|\Delta I_{NCL,r}\right| \tag{18}$$

Noting that

$$I_{NCL} = \frac{V_{S,N}}{R_{NCL}} cos\varphi_{SL} \tag{19}$$

and that

$$\begin{aligned} I_{NCL,a} &= I_{NCL}\ \cos\varphi_{SL} \\ I_{NCL,r} &= I_{NCL}\ \sin\varphi_{SL} \end{aligned} \tag{20}$$

it follows that:

$$\begin{aligned} \Delta I_{NCL,a} &= \frac{V_{S,N}}{R_{NCL}} (cos^2\varphi_{SL} - cos^2\varphi_{NCL}) \\ \Delta I_{NCL,r} &= \frac{V_{S,N}}{2R_{NCL}} [sin(2\varphi_{SL}) - sin(2\varphi_{NCL})] \end{aligned} \tag{21}$$

By (21), constraint (18) can be reformulated as

$$2\frac{|cos^2\varphi_{SL} - cos^2\varphi_{NCL}|}{|sin(2\varphi_{SL}) - sin(2\varphi_{NCL})|} > tan\varphi_G \tag{22}$$

where φ_G is the phase of the distribution line impedance

$$tan\varphi_G = \frac{X_G}{R_G} \tag{23}$$

The term at the left-hand side of (22) depends on the ES action while that on the right-hand side is a quantity characteristic of the distribution line supplying the RESE user. Eq. (22) represents the constraint to be met for ES to fulfill the demand-side power paradigm. For small excursions of φ_{SL} around the nominal conditions, eq. (22) simplifies in

$$|tan(2\varphi_{NCL})| > tan\varphi_G \tag{24}$$

which permits the a-priori check of the appropriateness of the ES action since it is independent of φ_{SL}.

V. ES STABILIZATION CAPABILITIES

By exploiting the equations in the previous Section, this Section determines the range of variations of the grid voltage which ES is able to cope with while fulfilling the demand-side power paradigm. Let us analyze first an R-line and then an RL-line.

A. R-LINE

The voltage drop in an R-line as a fraction of the nominal voltage drop is

$$\left.\frac{\Delta V_{DL}}{V_{DL,N}}\right|_{R-line} = \frac{\Delta I_{NCL,a}}{I_{G,a,N}} \tag{25}$$

By (10), (13), (14) and the twin equation of (13) for CL, eq. (25) can be rewritten as

$$\left.\frac{\Delta V_{DL}}{V_{DL,N}}\right|_{R-line} = \frac{1}{1+\frac{P_{CL,N}}{P_{NCL,N}}} \frac{\Delta P_{NCL}}{P_{NCL,N}} \tag{26}$$

Eq. (26) discloses that, for an R-line, the normalized value of ΔV_{DL} is equal to that of ΔP_{NCL} apart from a coefficient that is less and depends on the ratio $P_{CL,N}/P_{NCL,N}$. When $P_{CL,N}$ is much smaller than $P_{NCL,N}$, the plot of ΔV_{DL} coincides with that of $\Delta I_{NCL,a}$ in Fig. 7 and the ES stabilization capabilities, expressed in terms of the minimum and maximum values taken by ΔV_{DL} while ΔP_{NCL} ranges from $\Delta P_{NCL,Min}$ to $\Delta P_{NCL,Max}$, are exactly equal to -38% and to 23%. Eq. (26) also discloses that the ES stabilization capabilities are notably deteriorated when $P_{CL,N}$ is comparable to $P_{NCL,N}$, as illustrated in Fig. 8 where (26) is plotted for different values of the ratio $P_{CL,N}/P_{NCL,N}$. For instance, for a ratio equal to 1, ΔV_{DL} ranges only from -20 % to 11 %.

B. RL-LINE

The voltage drop in an RL-line as a fraction of the nominal voltage drop is

$$\left.\frac{\Delta V_{DL}}{V_{DL,N}}\right|_{RL-line} = \frac{R_G\,\Delta I_{NCL,a} + X_G \Delta I_{NCL,r}}{R_G\, I_{G,a,N} + X_G I_{G,r,N}} \tag{27}$$

By (10) and (21), eq. (27) can be rewritten as

$$\left.\frac{\Delta V_{DL}}{V_{DL,N}}\right|_{RL-line} = \frac{1+\frac{1}{2}tan\varphi_G \frac{sin(2\varphi_{SL}) - sin(2\varphi_{NCL})}{cos^2\varphi_{SL} - cos^2\varphi_{NCL}}}{1+tan\varphi_G tan\varphi_U} \frac{1}{1+\frac{P_{CL}}{P_{NCL,N}}} \frac{\Delta P_{NCL}}{P_{NCL,N}} \tag{28}$$

where φ_U is the phase of the total user impedance, given by the

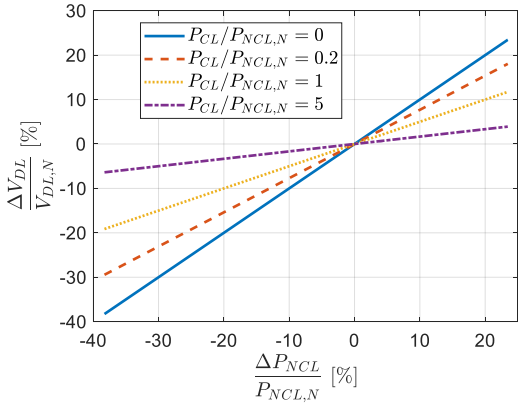

FIGURE 8. Line voltage drop vs. NCL-drawn active power (variational quantities) for different $P_{CL,N}/P_{NCL,N}$ ratios.

This article has been accepted for publication in a future issue of this journal, but has not been fully edited. Content may change prior to final publication. Citation information: DOI 10.1109/ACCESS.2020.3040292, IEEE Access

parallel of CL and NCL. Eq. (28) discloses that, for an RL-line, the normalized value of ΔV_{DL} depends on that of ΔP_{NCL} in a somewhat complex manner. Indeed, in addition to ratio $P_{CL,N}/P_{NCL,N}$ like for an R-line, it is affected by phase φ_U, which is a fixed quantity for a given user, by phase φ_{SL}, which is a quantity that changes with ΔP_{NCL}, and by phase φ_G, which is also a fixed quantity for a given distribution line.

Let i) CL and NCL have the same phase so that it is $\varphi_U = \varphi_{NCL}$, and ii) $P_{CL,N}$ be much smaller than $P_{NCL,N}$. For low values of ΔP_{NCL}, eq. (28) becomes independent on phase φ_{SL}, as given by

$$\left.\frac{\Delta V_{DL}}{V_{DL,N}}\right|_{RL-line} = \frac{1-\frac{tan\varphi_G}{|tan(2\varphi_{NCL})|}}{1+tan\varphi_G tan\varphi_{NCL}} \frac{\Delta P_{NCL}}{P_{NCL,N}} \qquad (29)$$

This expression confirms that the ES stabilization fulfils the demand-side power paradigm as long as (24) is met because only then do ΔV_{DL} and ΔP_{NCL} have the same sign.

C. RL-LINE STABILIZATION CAPABILITIES

For an RL-line, the key equation governing the user voltage stabilization is (28). To discuss the impact of the phase of the distribution line impedance on a stabilization fulfilling the demand-side power paradigm, reference is made to a user with $cos\varphi = 0.9$, for both CL and NCL, and $P_{CL,N} << P_{NCL,N}$; moreover, RL-lines with different $tan\varphi_G$ are considered. Note that, for $cos\varphi = 0.9$, the constraint in (24) becomes $1.26 > tan\varphi_G$.

Fig. 9 (a) plots (28) for some values of $tan\varphi_G$ less than 1.26; they stand out for the substantial prevalence of the resistive component in the distribution line impedance. The curves demonstrate that ES is able to stabilize the user voltage and to the fulfill the demand-side power paradigm. They also establish that, under the demand-side power paradigm,

i. the stabilization capabilities reduce as the ratio of the line reactance component to the resistance one, and hence $tan\varphi_G$, increases; indeed, the maximum and minimum values taken by ΔV_{DL} within the allowable range of ΔP_{NCL} decrease; furthermore, the maximum is reached for ΔP_{NCL} lower than $\Delta P_{NCL,Max}$,
ii. as $tan\varphi_G$ increases, there is no user voltage stabilization beyond certain positive values of ΔP_{NCL} since ΔV_{DL} becomes negative,
iii. for $tan\varphi_G = 1.26$, the user voltage stabilization is possible only for negative values of ΔP_{NCL}.

Fig. 9 (b) plots (28) for some values of $tan\varphi_G$ greater than 1.26; they stand out for the substantial prevalence of the reactive component in the distribution line impedance. At a first glance it turns out that there is no user voltage stabilization with the fulfilment of the demand-side power paradigm around $\Delta P_{NCL} = 0$, as predicted by (29). Moreover, there is no chance of stabilizing the user voltage for positive values of ΔP_{NCL}. Instead, an interval exists in the negative

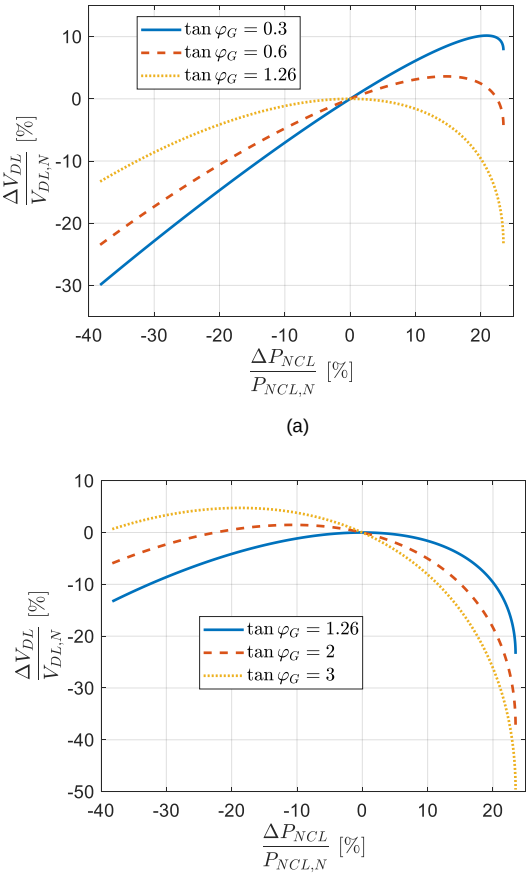

FIGURE 9. Line voltage drop vs. NCL-drawn active power (variational quantities) for (a) $1.26 \leq tan\varphi_G$**, (b)** $1.26 \geq tan\varphi_G$.

range of ΔP_{NCL}, where -below certain values of ΔP_{NCL}- the user voltage can be stabilized even for $tan\varphi_G < 1.26$. Since ΔV_{DL} is limited in magnitude and the interval is located at the border of the negative range of ΔP_{NCL}, this stabilization capability is of poor practical interest. Lastly, by increasing $tan\varphi_G$ beyond 3 there is no stabilization chance under the demand-side power paradigm even for negative values of ΔP_{NCL}.

It is worth to note that the user voltage can still be stabilized for strongly inductive lines, i.e. with $tan\varphi_G = 3$ or greater. The fundamental achievement of the analysis above is that the stabilization is here reached with NCL drawing an active power that varies exactly in the opposite direction to that required by the demand-side power paradigm; specifically, by decreasing the active power drawn by NCL under a grid overvoltage and by its increasing under a grid undervoltage. This behavior is at odds with the rule of adapting the load power demand to the generation, which is preferable paradigm for a grid with a large power generation from RESs.

VI. CASE STUDY EXEMPLIFICATION AND TESTING

This article has been accepted for publication in a future issue of this journal, but has not been fully edited. Content may change prior to final publication. Citation information: DOI 10.1109/ACCESS.2020.3040292, IEEE Access

Theoretical findings of the paper are exemplified and tested for a case study that consists of a single-phase user supplied by a low-voltage (LV) distribution line. Data of the case study are reported in Tab. II and are representative of a typical domestic European utility. Inspection of Tab. II points out that both CL and NCL are resistive-inductive loads with a power factor of 0.9 and that they together draw an overall power of 6 kW with a power share between NCL and CL of 5 to 1. The LV distribution line has $tan\varphi_G = 0.3$, which is a common value for small-section line conductors. The line impedance is 1 Ω, meaning that the grid is somewhat weak and justifies the adoption of ES for the user supply voltage stabilization.

Exemplification is carried out by using (28) to calculate the variations (V_G-$V_{G,N}$) of the grid voltage that ES is able to stabilize as a function of the variation of the active power drawn by NCL. The calculated results are plotted with solid blue line in Fig. 10 and show that the user voltage is stabilized against grid voltage variations ranging from -7 to 2.1 V; at the two extremities of the range, there are respectively a lack of 1800 W and a surplus of about 1000 W in the power drawn by NCL, with the lack that is about 5.5% greater and the surplus that is about 15% less than the respective minimum/maximum values calculated from Tab. I.

Testing is executed by simulating the circuit of Fig. 2 with the Power toolbox in the Matlab/Simulink environment. Two operating limits have been set for the ES operation, namely i) under grid undervoltage, the minimum power drawn by NCL is set at 3.2 kW in accordance with Tab. I, and ii) under grid overvoltage, the ES action is stopped once its action is no more able to stabilize the user supply voltage.

The simulation results are shown in Fig. 10 by means of red crosses and agree very well with the calculated ones. As an additional exemplification and test, calculated and simulation results are obtained for a LV distribution line with the same impedance but supposing that its $tan\varphi_G$ is equal to 0.7. The results are shown in Fig. 10 with the dashed blue line and the green crosses, respectively. Matching of the results also here substantiates the soundness of the theoretical findings.

TABLE II
CASE STUDY DATA

Parameter	Value
CL Nominal Voltage ($V_{S,N}$)	230 V
CL Nominal Active Power (P_{CL})	1 kW
CL Power Factor ($cos\varphi_{CL}$)	0.9
CL Impedance (Z_{CL})	47.6 Ω
CL Resistance (R_{CL})	42.9 Ω
CL Reactance (X_{CL})	20.7 Ω
NCL Nominal Active Power ($P_{NCL,N}$)	5 kW
NCL Power Factor ($cos\varphi_{NCL}$)	0.9
NCL Impedance (Z_{NCL})	9.5 Ω
NCL Resistance (R_{NCL})	8.6 Ω
NCL Reactance (X_{NCL})	4.2 Ω
LV Distribution Line Impedance (Z_G)	1 Ω
LV Distribution Line $tan\varphi_G$	0.3

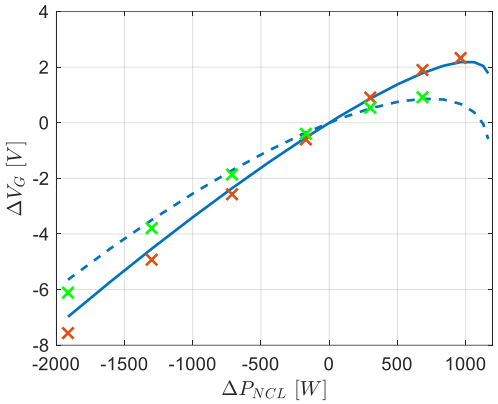

FIGURE 10. Stabilized grid voltage vs. NCL-drawn active power for the case study.

VII. CONCLUSIONS

Stabilization of the user voltage against the grid voltage variations by means of ES is extensively studied in the literature, but without paying attention to the ensuing variations in the active power drawn by NCL. This in spite of the fact that the grid voltage variations are normally caused by the fluctuations in the power generation, especially in the grids fed by RESs. Indeed, an excess in the power generation produces a grid overvoltage and, vice versa, a shortage in the power generation produces a grid undervoltage. Thus, an ES action that would force the power drawn by NCL in the opposite direction with respect to the power generation stands in the way of the correct functioning of an electric system.

To face this issue, operation and stabilization capabilities of a reactive ES has been analyzed on the basis of the demand-side power paradigm, by imposing that the active power drawn by NCL tracks the power generation. The analysis has been conducted in terms of normalized quantities so that the theoretical findings cover any RESE user, irrespective of the application context.

The significant outcomes of the analysis can be summarized as follows: i) only a distribution line with a resistive component of its impedance is able to give ES the capabilities of stabilizing the user voltage while fulfilling the demand-side power paradigm, ii) the presence of a reactive component in the distribution line impairs such capabilities, until to cancel them out when the reactive component dominates. The outcomes are supported by the formulation of the constraint for the paradigm to be fulfilled and the investigation of the impact of the user and distribution line parameters on the constraint.

Lastly, a numerical exemplification of the theoretical findings has been given for the case study of a typical RESE user connected to a LV distribution line. The calculated results

have been validated by simulating the case study in the Matlab/Simulink environment.

REFERENCES

[1] S. Hashemi and J. Ostergaard, "Methods and strategies for overvoltage prevention in low voltage distribution systems with PV," *IET Renew. Power Gen.*, vol. 11, no. 2, pp. 205–214, 2017.

[2] J. Hu, Z. Li, J. Zhu and J. M. Guerrero, "Voltage Stabilization: A Critical Step Toward High Photovoltaic Penetration," *IEEE Ind. Electron. Mag.*, vol. 13, no. 2, pp. 17-30, Jun. 2019.

[3] S. Y. R. Hui, C. K. Lee, and F. F. Wu, "Electric springs—a new smart grid technology," *IEEE Trans. Smart Grid*, vol. 3, no. 3, pp. 1552–1561, Sep. 2012.

[4] C. K. Lee, S. C. Tan, F. F. Wu, S. Y. R. Hui and B. Chaudhuri, "Use of Hooke's law for stabilizing future smart grid — The electric spring concept," in Proc. of Energy Convers. Conf. & Expo., 2013, pp. 5253-5257.

[5] Q.Wang, F.Deng, M.Cheng and G.Buja, "The State of the Art of Topologies for Electric Springs", *Energies*, vol. 11, no. 7, pp. 1-21, Jul. 2018.

[6] N. R. Chaudhuri, C. K. Lee, B. Chaudhuri and S. Y. R. Hui, "Dynamic Modeling of Electric Springs," *IEEE Trans. Smart Grid*, vol. 5, no. 5, pp. 2450-2458, Sep. 2014.

[7] S. Giacomuzzi, G. Buja, M. Bertoluzzo and Q. Wang, "Dynamic Behavior Analysis and Control of Reactive Electric Springs," in Proc. 29th IEEE International Symposium on Industrial Electronics (ISIE), 2020, pp. 833-838.

[8] S. Tan, C. K. Lee and S. Y. Hui, "General Steady-State Analysis and Control Principle of Electric Springs With Active and Reactive Power Compensations," *IEEE Trans. Power Electron.*, vol. 28, no. 8, pp. 3958-3969, Aug. 2013.

[9] J. Soni and S. K. Panda, "Electric Spring for Voltage and Power Stability and Power Factor Correction," *IEEE Trans. Ind. App.*, vol. 53, no. 4, pp. 3871-3879, Jul.-Aug. 2017.

[10] Q. Wang, M. Cheng, Y. Jiang and W. Zuo and G.Buja, "A Simple Active and Reactive Power Control for Applications of Single-Phase Electric Springs", *IEEE Trans. Ind. Electron.*, vol. 65, no. 8, pp. 6291-6300, Aug. 2018.

[11] C. Yuan, M. Tong, J. Feng and R. Zhou, "Control of electric spring for frequency regulation," *J. Eng.*, vol. 2019, no. 16, pp. 2500-2504, Mar. 2019.

[12] C. Lee, H. Liu, S. Tan, B. Chaudhuri and S. Y. Hui, "Electric Spring and Smart Load: Technology, System-level Impact and Opportunities," *IEEE Trans. Emerg. Sel. Topics Power Electron.*, doi: 10.1109/JESTPE.2020.3004164.

[13] S. Yan, C. K. Lee, T. Yang, K. T. Mok, S. C. Tan, B. Chaudhuri, and S. Y. R. Hui, "Extending the operating range of electric spring using back-to-back converter: Hardware implementation and control," *IEEE Trans. Power Electron*, vol. 32, no. 7, pp. 5171–5179, Jul. 2017.

[14] T. Yang ; K. Mok ; S. Ho ; S.C. Tan ; C.K. Lee ; S.Y.R. Hui, "Use of integrated photovoltaic-electric spring system as a power balancer in power distribution networks", *IEEE Trans. Power Electron.*, vol. 34, No. 6, pp 5312 – 5324, Jun. 2019.

[15] Y. Zheng, W. Kong, Y. Song and D. J. Hill, "Optimal Operation of Electric Springs for Voltage Regulation in Distribution Systems," *IEEE Trans. Ind Informat.*, vol. 16, no. 4, pp. 2551-2561, Apr. 2020.

[16] L. Liang, Y. Hou and D. J. Hill, "Enhancing Flexibility of an Islanded Microgrid With Electric Springs," *IEEE Trans. Smart Grid*, vol. 10, no. 1, pp. 899-909, Jan. 2019.

[17] A. K. Khamis, N. E. Zakzouk, A. K. Abdelsalam and A. A. Lotfy, "Decoupled Control Strategy for Electric Springs: Dual Functionality Feature," *IEEE Access*, vol. 7, pp. 57725-57740, 2019.

[18] D. Chakravorty, J. Guo, B. Chaudhuri and S. Y. R. Hui, "Small Signal Stability Analysis of Distribution Networks With Electric Springs," *IEEE Trans. Smart Grid*, vol. 10, no. 2, pp. 1543-1552, Mar. 2019.

[19] L. Liang, H. Yi, Y. Hou and D. J. Hill, "An Optimal Placement Model for Electric Springs in Distribution Networks," *IEEE Trans Smart Grid*, doi: 10.1109/TSG.2020.3011957.

[20] Y. Zheng, D. J. Hill, Y. Song, J. Zhao and S. Y. R. Hui, "Optimal Electric Spring Allocation for Risk-Limiting Voltage Regulation in Distribution Systems," *IEEE Trans. Power Syst.*, vol. 35, no. 1, pp. 273-283, Jan. 2020.

[21] T. Chen, J. Guo, B. Chaudhuri and S. Y. Hui, "Virtual Inertia From Smart Loads," *IEEE Trans. Smart Grid*, vol. 11, no. 5, pp. 4311-4320, Sep. 2020.

[22] Z. Akhtar, B. Chaudhuri and S. Y. R. Hui, "Smart Loads for Voltage Control in Distribution Networks," *IEEE Trans. Smart Grid*, vol. 8, no. 2, pp. 937-946, Mar. 2017.

[23] *Electrical Installations for Buildings*, IEC 60364, 2005.

Giuseppe Buja (M'75–SM'84–F'95–LF'13) received the 'Laurea' degree with honors in power electronics engineering from the University of Padova, Padova, Italy, where he is currently an Honorary Research Scientist.

He has carried out pioneering research works in the field of power and industrial electronics, originating the modulating-wave distortion and the optimum modulation for pulse-width modulation inverters, initiating the application of digital signal processors to the control systems of power electronics converters, and conceiving advanced techniques for the control of electric drives. In the last years, he turned his research interests towards the automotive electrification, including wireless charging of electric vehicles, and grid-integration of renewable energy sources.

Dr. Buja received the IEEE Industrial Electronics Society (IES) Eugene Mittelmann Achievement Award "in recognition of his outstanding technical contributions to the field of industrial electronics," and the 2016 Best Paper Award from the IEEE Transactions on Industrial Electronics. He has served the IEEE in several capacities, including as the General Chairman of the 20th Annual Conference of IES (IECON'94) and an Associate Editor of the IEEE Transactions on Industrial Electronics. At present, he is a member of International Conference Steering/Technical Committees and Scientific Journal Editorial Boards, and a Senior Member of the Administrative Committee of IES.

Stefano Giacomuzzi (S'17) was born in Este, Padova, Italy, in 1991. He received the B.S. degree in Energy Engineering and M.S. degree in Electrical Engineering from the University of Padova, Padova, Italy, in 2013 and 2016, respectively. In 2016 he received a research grant for the research project "AC Electric Energy Hub" at the Department of Industrial Engineering, University of Padova. He is currently working at the same department on his Ph.D degree. His research interests include power electronics circuits and control systems for renewable energy sources, microgrids management and smart transformers applications.

Qingsong Wang (S'14–M'17–SM'17) received the B.Sc. and M.Sc. degrees from the Department of Electrical Engineering, Zhejiang University, Hangzhou, China, in 2004 and 2007, respectively, and the Ph.D. degree from the School of Electrical Engineering, Southeast University, Nanjing, China, in 2016. From November 2015 to November 2016, he was a joint Ph. D student with the Department of Energy Technology, Aalborg University, Aalborg, Denmark, where he focused on electric springs.

From July 2004 to July 2005, he was an engineer in Shihlin Electronic & Engineering Co., Ltd, Suzhou, China. From July 2007 to August 2011, he was an engineer in Global Development Center of Philips Lighting Electronics, Shanghai, China. In October 2010, he was promoted to be a Senior Engineer. From August 2011 to September 2013, he was a Lecturer

in PLA University of Science and Technology, Nanjing, China. Since 2017, he has been with Southeast University, where he is currently a he is currently an Associate Professor in the School of Electrical Engineering. He is also with Jiangsu Key Laboratory of Smart Grid Technology and Equipment.

Dr. Wang's research interests are focused in the areas of control and applications of power electronics to power systems.

Manuele Bertoluzzo received the M.S. degree in electronic engineering and the Ph.D. degree in industrial electronics and computer science from the University of Padova, Padova, Italy, in 1993 and 1997, respectively. From 1998 to 2000, he was a member of the Research and Development Division of an electric drive factory. In 2000, he joined the Department of Electrical Engineering, University of Padova, as a Researcher in the Scientific Disciplines' Group "electric converters, machines, and drives." Since 2015 he is Associate Professor and hold the lectureships of Road Electric Vehicles and Systems for Automation for the students of the master's degree in Electric Engineering. He is currently involved in the analysis and design of power electronics systems, especially for the wireless charging of electric vehicles battery.